Pozo Garcia, Octavio; Tikkala, Vesa-Matti; Zakharov, Alexey; Jämsä-Jounela, Sirkka-Liisa

Integrated FDD system for valve stiction in a paperboard machine

Published in:
Control Engineering Practice

DOI:
10.1016/j.conengprac.2013.02.014

Published: 01/01/2013

Document Version
Peer-reviewed accepted author manuscript, also known as Final accepted manuscript or Post-print

Please cite the original version:
Pozo Garcia, O., Tikkala, V.-M., Zakharov, A., & Jämsä-Jounela, S.-L. (2013). Integrated FDD system for valve stiction in a paperboard machine. *Control Engineering Practice*, *21*(6), 818-828.
https://doi.org/10.1016/j.conengprac.2013.02.014

Author's accepted manuscript, published in Control Engineering Practice 21(6) 818-828, 2013

Integrated FDD system for valve stiction in a paperboard machine

Octavio Pozo Garcia* Vesa-Matti Tikkala* Alexey Zakharov* Sirkka-Liisa Jämsä-Jounela*

**Aalto University School of Chemical Technology,*
Department of Biotechnology and Chemical Technology
P.O. Box 16100, 00076 Aalto
Finland (e-mail: octavioado@gmail.com*)*
Fax: +358 - 9 - 470 23846

Abstract: The performance of a modern industrial plant can be severely affected by the performance of its key devices, such as valves. In particular, valve stiction can cause poor performance in control loops and can consequently lower the efficiency of the plant and the quality of the product. This paper presents an integrated FDD system for valve stiction which employs various FDD methods in a parallel configuration. A reliability index was integrated into each method in order to estimate their degree of influence in the final diagnosis of the system. Each method and the integrated system were tested using industrial data.

Keywords: Fault detection and diagnosis, valve, oscillations, shape analysis, stiction, industrial application

1 Introduction

A process plant aims to deliver a product with specific quality characteristics and to simultaneously maintain efficient process operation. This can be achieved by avoiding situations, such as loss of production time or waste of resources caused by faults in the process devices. Valves are one of the most common devices in the process industry; they are used in a wide scope of tasks, and they can be the only actuating part of a control loop in some applications. In some specific cases, valve faults can negatively affect the performance of an entire plant. Valve faults may arise due to an increase in its minimum opening (leakages), due to a higher than normal difference between the objective valve output and the real output (hysteresis, clogging), and due to static friction (stiction). Stiction in particular has been found to be a frequent reason for poor performance of control loops (Ender, 1993). A valve under stiction should be repaired or replaced immediately. However, replacement of the valve would normally interrupt the process completely. Moreover, in most cases, stiction is not discovered due to the high number of devices and control loops present in the plant. Therefore, the development and implementation of automated fault detection and diagnosis systems for valves has become necessary to improve the efficiency of process plants.

Fault detection in valves is typically based on supervision of the available measured variables (Isermann, 2011). Therefore, most methods can only detect the presence of a specific fault type. To avoid this limitation, special sensors can be installed in valves. For example, a method presented by Kano (2004) is based on the difference between valve position and controller output. However, due to economic or operational issues these sensors are rarely used in industrial plants. Currently there are several types of fault detection and diagnosis (FDD) methods which do not require the installation of new equipment. Jelali and Huang (2010) have reviewed the most common methods for detecting and diagnosing valve stiction discussed in the literature, most of which recognize special characteristics of control-related signals

In the shape-based methods, the analyzed characteristic is the shape of the control-related signals. In other methods, the nonlinearity of the signals is evaluated. Alternatively, there are direct methods which employ first principle valve models, while some methods use system identification techniques to determine stiction parameters.

Among the methods which utilize the characteristics of the monitored signals, a method based on the cross-correlation function between the controller output and the controlled variable is presented by Horch (1999). It is assumed that the cross-correlation function is even if the loop is free of stiction, whereas an odd function is indicative of stiction in the valve. Stenman, Gustafsson, and Forsman (2003) presented a method which utilizes a segmentation model to identify a sequence of jumps in the valve position.

Among the shape-based methods, Kano, Maruta, Shimizu, and Kugemoto (2004) presented a stiction detection technique based on the difference between the shape produced by sinusoidal oscillations and the shape of oscillations caused by stiction. Singhal et al. (2005) proposed a method based on the symmetry of the oscillation signal produced by a healthy control loop. In this method the area of each half-period of the analyzed signal is calculated in order to construct an index of the symmetry of the signal. Yamashita (2006) utilized the shapes of the input-output plots during oscillations to identify parameters related to stiction. Scali et al. (2008) introduced a method based on the similarity between the shape of the oscillation caused by stiction and by relay control. In this method a signal generated by a relay model and sinusoidal and triangular functions are matched to the controlled signal. In cases where the triangular function or the relay signal exhibit a closer fit to the controlled variable stiction can be recognized in the control loop. Hägglund (2011) presented a method where rectangular and sinusoidal signals are matched to the control error. A loss function, based on the integral absolute error (IAE), is used to evaluate the matching quality.

Among the methods analyzing nonlinearity of a signal, Choudhury et al. (2006) introduced a technique for detecting the presence of nonlinearity in a control loop. If nonlinearity is detected, a phase plot is constructed using input-output data.

Stiction is identified if the shape of the plot has an elliptical pattern. Another method introduced by Thornhill (2005), employed surrogate data analysis to detect nonlinearity in the control loop. If the presence of process nonlinearity and non-linear disturbances is excluded, any detected nonlinearity can be related to valve stiction.

Among the methods which employ system identification techniques, Srinivasan et al. (2005) and Lee et al. (2008) proposed similar approaches, where the main idea is parameter identification of the non-linear part of a Hammerstein model to diagnose stiction. The difference between the methods is in their identification algorithm and the structure of the linear part of the Hammerstein model. Nallasivam et al. (2010) presented a technique based on the identification of the parameters of a Volterra model. If the Fourier transform of the model exhibits many harmonic components, this indicates that the loop is under stiction.

Comparative studies of the valve stiction diagnosis have been given by Rossi and Scali (2005), Horch (2006), and Jelali and Scali (2010). All of which have conclude that there is no individual technique capable to diagnose all possible types of stiction features. Moreover, research should focus on analyzing the methods and their possible combinations (Jelali and Scali, 2010). Recently, Scali and Farnesi (2010) have proposed a control loop monitoring system, in which stiction diagnosis is achieved by selecting between stiction detection algorithms according to control loop characteristics. However, research on integrating the diagnosis of different algorithms is still scarce.

The aim of this paper is to present an integrated FDD system for valve stiction using a parallel configuration of the most common algorithms for stiction detection; in order to improve the reliability of the diagnosis decision on industrial environments. For this purpose, the use of integrated diagnosis index and separate reliability indices for each detection method are proposed. The paper also includes the testing results and a comparison analysis of each stiction algorithm using industrial paperboard machine data. The paper is organized as follows: Section 2 describes the board machine, its critical faults and the problem of stiction. Section 3 presents the structure of the proposed integrated FDD system, the implemented valve stiction diagnosis methods, and their reliability indices. Section 4 describes the testing procedure and study cases. Section 5 presents the tests results of each stiction diagnosis algorithm and the integrated system. Additionally, the performances of the individual diagnosis algorithms and the integrated system are compared. In the final section, the conclusions of this work are presented and discussed.

2 Case Process

2.1 Paperboard machine process

The case process, a paperboard machine, produces three-layer uncoated liquid packaging boards and cup boards. The raw materials are hardwood and softwood kraft pulps, chemi-thermomechanical pulp (CTMP) and broke. The board making process is composed of six different sections. In the stock preparation section, the raw material used in the board machine is prepared. The process of forming the web starts in the wire section, in which the material flow from the stock preparation is spread on the wire. Next, in the press section, the water is removed from the web by applying mechanical force. In this section it is also possible to control some of the thickness and surface properties of the board. In the drying section, the final moisture content of the board is achieved. The final characteristics of the surface properties such as, gloss, smoothness, and thickness of the board, are achieved in the calendaring section. The final section of the board machine is the reeling and delivery section. The main objective of a board machine is to produce board with properties that satisfy the requirements set by the producer and the end client. It is important to notice that in board making, one of the main quality characteristics is the product uniformity. Thus, quality variables such as basis weight, moisture, and thickness require monitoring and control. The control system in the board machine is composed of three layers. The supervisory layer is the quality control system (QCS). It monitors the quality variables and provides set points for the controllers of the lower layer, the stabilizing control layer. The basic control layer consists of all the individual control loops required for running the process devices

A comprehensive fault analysis of the board machine was performed based on the operational and maintenance data of the year 2010. The aim of the study was to determine the fault types in the machine and the devices most affected by them. One of the most important findings of the study was the discovery that valves were one of the most critical devices in the process. Moreover, the maintenance reports showed stiction to be the main cause for the valve malfunctioning. Table 1 shows the main fault types and faulty devices, as found in the fault analysis reported by Jämsä-Jounela et al. (2012).

Table 1: Basic control layer devices and fault types

	Clogging, jamming	Leakage	Loosening, disengagement	Malfunction	Other damage	Overheating	Vibration	Total
Drive	0,63	-	-	5,06	1,90	0,63	0,63	8,86 %
Hydraulic device	1,90	9,49	1,27	1,90	5,70	0,63	-	20,89 %
Inverter	-	-	-	4,43	2,53	-	-	6,96 %
Other mechanical device	3,80	1,27	3,80	3,80	4,43	-	-	17,09 %
Pump	2,53	8,23	0,63	1,27	1,90	1,27	3,80	19,62 %
Sensor	-	0,63	1,27	7,59	-	-	-	9,49%
Valve	-	3,80	1,27	12,03	-	-	-	17,09 %
Total	8,86 %	23,42 %	8,23 %	36,08 %	16,46 %	2,53 %	4,43 %	100,00 %

2.2 Valve stiction

A valve under stiction operates with less efficiency, meaning that its response time, energy consumption, and operation region will change. Valve stiction is typically caused by several factors, such as seal degradation, lack of lubricant, contamination by solid material, and tightening of the packing in the valve body. Physically identifying stiction can be a difficult task. The effects and magnitude of stiction can vary according to time and operating conditions. In addition, the frictional force in many valves can change according to their position. For example, in some valves the friction is higher when the valve opens than when it closes. Nevertheless, from the control loop perspective stiction introduce cycling and variability, thus severely affecting the performance of the loop. Figure 1 illustrates the effects of stiction on valve operation.

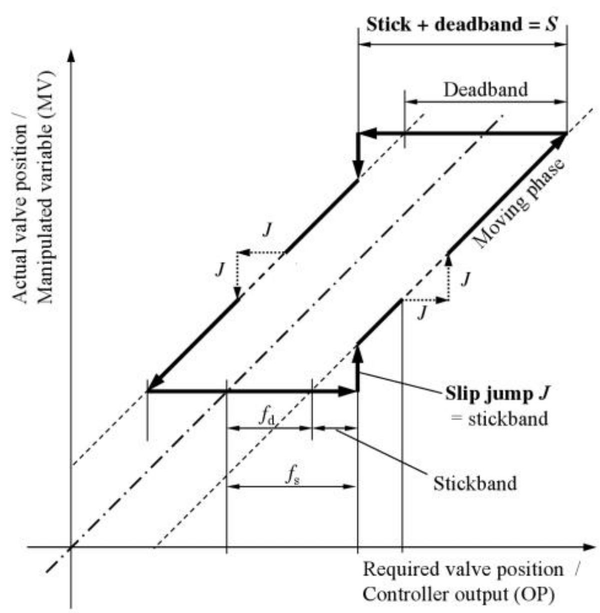

Figure 1: Effect of stiction in valve operation

In a control loop, the cycling nature of stiction commonly translates into oscillating behavior since stiction delays the normal movement of the valve while the process input remains constant. Consequently, the controller error increases, which forces the controller output to change until the valve overcomes the friction. This then causes the valve to slip and the process output to change beyond its set point (see Fig. 1). This behavior repeats until the valve is replaced or serviced. Figure 2 shows this behavior as it was observed in a pressure control valve in the drying section of the paperboard machine.

Oscillations generated by valve stiction can propagate to different parts of the paperboard machine. This is a direct consequence of the tight interconnection between its sections. Ultimately, these oscillations may affect the quality variables in the board machine, degrading the performance of the process and the quality of the product. Figure 3 shows the power spectra of the pressure control loops in the drying groups of the board machine. Several drying groups exhibit a peak at the same frequency in the spectra, which is actually the same frequency observed in the loop affected by stiction in the second drying group.

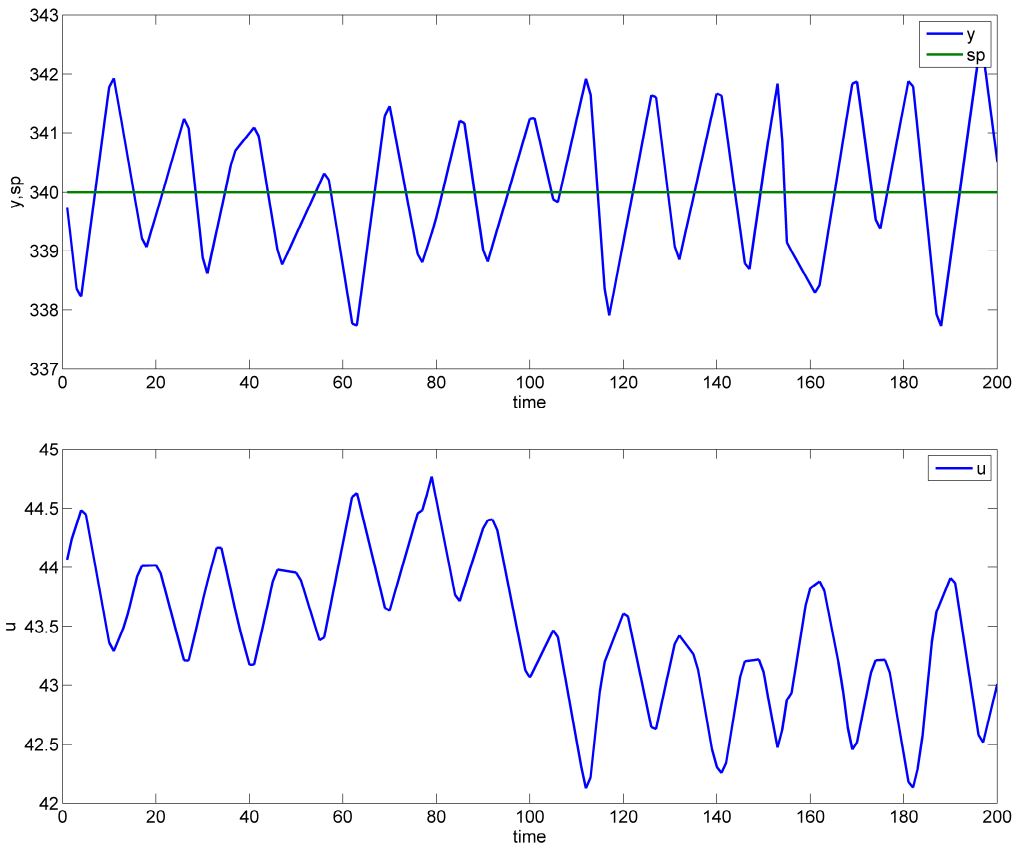

Figure 2: Stiction behavior in a pressure valve (top) and its effect in the controller output (bottom) on the board machine.

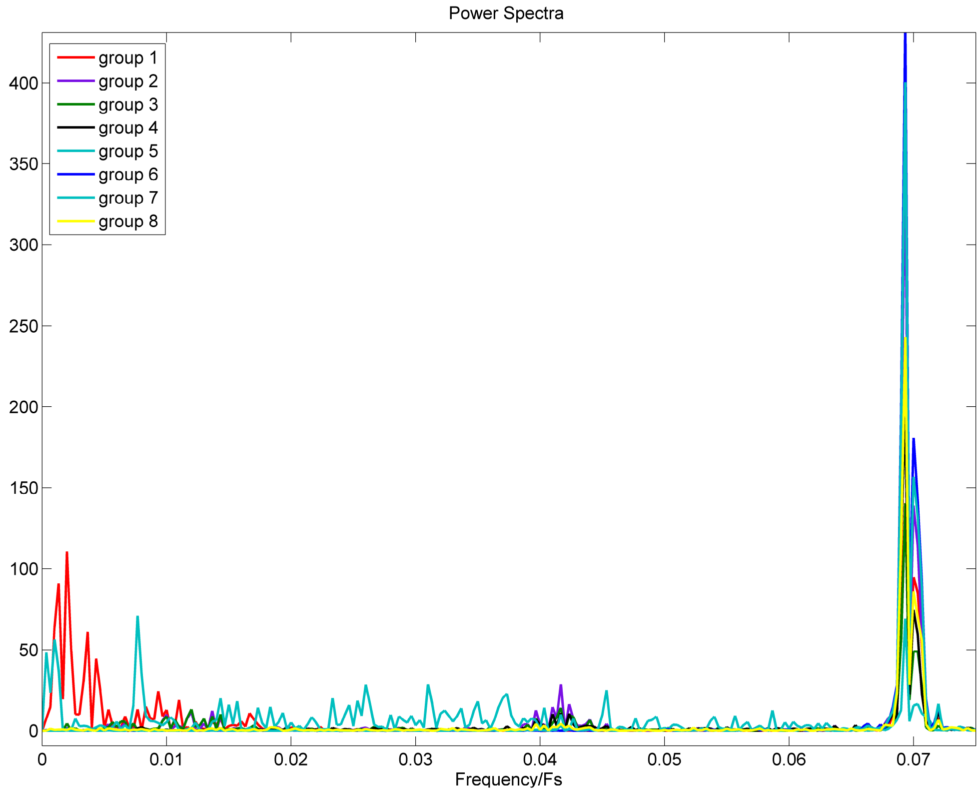

Figure 3: The power spectra of the drying groups during a period when a pressure valve is under stiction.

3 Integrated FDD System for Valve Stiction

The integrated FDD system, developed in this study, employs a parallel configuration, where the most common valve stiction diagnosis methods were implemented concurrently. A reliability index was integrated into each method defining their degree of influence in the final diagnosis. In this manner, all methods contributed to the final diagnosis decision, improving the reliability of the results and avoiding an ambiguous or contradictory diagnosis.

The integrated FDD system for valve stiction consists of the following phases: first data preprocessing during which tasks such as verifying the sampling time and removing outliers, large disturbances, and gaps in the data are performed; second, calculation of the stiction indices; third, calculation of the reliability indices; and the final phase in which the integrated diagnosis decision is achieved. The entire procedure is illustrated in Figure 4.

The FDD methods used in the integrated system are the histogram method (Horch, 2006), the curve fitting method (He et al., 2007), the rectangular fitting method (Hägglund, 2011), and the bicoherence method (Choudhury, 2006): The first three methods base their diagnosis on the shape of a signal, or in case of Horch's method, its histogram and the fourth method is based on evaluating the nonlinearity of a process signal.

3.1 Histogram method

Horch (2006) presented the histogram method for stiction detection in valves. The method is based on identifying abrupt changes in the process by computing the second derivative for an integrating processes, or the first derivative for self-regulating processes, of the controlled output *y(t)*. If *y(t)* exhibits a triangular shape during oscillations, the analyzed derivative will show a signal resembling a pulse train signal. If the pulse train is neglected and additional Gaussian noise is assumed, the analyzed derivative will have a normal or close to normal probability distribution. If there is no stiction present, the oscillating signal *y(t)* will have a sinusoidal shape. In consequence, the probability distribution of the analyzed derivative will have two separate maxima. Therefore, in order to perform the detection decision, the probability distribution of the second derivative is tested against two probability distributions (normal and camel distributions).

The first step of the algorithm is to filter and differentiate the signal. The filter has to attenuate the noise without significantly affecting the shape of the oscillation. The whole filtering and differentiation procedure can be summarized as follows:

$$y_{df}(t) = \left(\frac{(1-\alpha)(1-q^{-1})}{1-\alpha q^{-1}}\right)^2 y(t) \qquad (1)$$

where $y_{df}(t)$ is the filtered second derivate of the process output, and α is a filter design parameter. Next, a normalized sample histogram of $y_{df}(t)$ is obtained. According to Bendat (1971), the number of histogram classes K for datasets of more than N = 2000 samples can be determined as $K = 1.37(N-1)^{0.4}$. To calculate the stiction index, a Gaussian distribution and a camel distribution are fitted to the sample histogram of $y_{df}(t)$. The Gaussian distribution is defined as

$$f_G(x) = \frac{1}{\sqrt{2\pi\sigma}} exp \frac{-(x-\mu)^2}{2\sigma^2} \qquad (2)$$

whereas the camel distribution is defined as

$$f_Z(z) = \frac{1}{\sigma\sqrt{2\pi}} \int_{-A}^{A} \frac{\exp\left(-\frac{(z-x-\mu)^2}{2\sigma^2}\right)}{\sqrt{A^2-x^2}} dx \qquad (3)$$

The amplitude A can be estimated from the data, and the parameter σ is used to fit the distribution to the sample histogram:

$$\hat{\sigma} = \arg\min \sum \left[f_z\left(z,\sigma\right) - Y \right]^2 \qquad (4)$$

where Y is the data from the sample histogram.

Once the fitting procedure has been performed for both distributions, the mean squared errors can be calculated. If the fit for the Gaussian distribution is better, stiction is determined to be present in the loop. In this method, the stiction index I_H=0 if there is no stiction and I_H=1 if stiction is present. If both fits are approximately similar, the method is unable to provide a diagnosis decision. As can be seen, the main problem with the stiction index calculation is that it only identifies which fitting error is lower. Therefore, if the fitting is similarly good for both distributions, the method is unable to provide a diagnosis decision. Moreover, if the fittings of both probabilities are poor, the method would not give any indication of uncertainty as long as one of the fitting errors is significantly lower than the other.

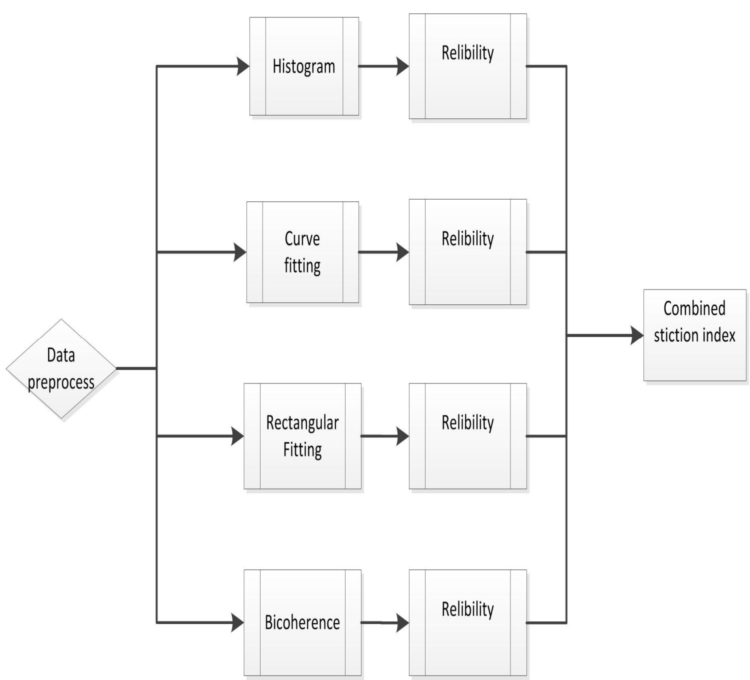

Figure 4: Integrated FDD system flow chart

3.2 Curve fitting method

The curve fitting method (He et al., 2007) is based on the assumption that, for integrating processes, the controlled variable (CV) signal has the shape of a triangular wave when stiction is present. In contrast, if there is no stiction, the shape of the CV signal will exhibit a sinusoidal behavior. Thus, two different functions (triangular and sinusoidal) are fitted to the measured oscillating signal and compared. The results given by the method are presented in the stiction index I_C, which serves the dual purpose of indicating and quantifying the stiction in the loop. In case the process is self-regulating the controller output should be analyzed.

The first step of the method is to locate the zero-crossings in the signal. With this information, the half-periods of the oscillating signal are identified. Next, the fitting of the triangular and sinusoidal functions can be performed.

Next, the sinusoidal function is fitted piece-wise for each half-period of oscillations using the least-squares method and its mean-squared error $\mathrm{MSE}_{\sin}$ is calculated. The triangular fitting is slightly more demanding since it requires a piecewise curve fitting with two degrees of freedom (the location and magnitude of the maxima of each period.) In order to calculate the best fitting, it is necessary to use a numerical iterative method.

The triangular fitting algorithm consists of the following steps:

1. For each half-period of the signal set the minimum mean squared error as MSE(i)≈∞

2. For the peak location t_p in the period represented by t_i and t_{i+1}, first find the linear least square fit for $t_i : t_p$, with the constraint that the triangular signal has to pass the first zero crossing point at t_i,

3. Find the linear least square fit for $t_{p+1} : t_{i+1}$ (the second half of the period), with the constraint that the rectangular signal has to pass the second zero crossing point at t_{i+1}.

4. Finally calculate the MSE between t_i and t_{i+1}.

5. Repeat steps 2 to 4 for different peak locations.

The final step of the algorithm is to calculate the I_C, the stiction index, which is defined as the ratio of the MSE of the sinusoidal fit to the summation of the MSEs of both sinusoidal and triangular fits.

$$I_C = \frac{\mathrm{MSE}_{\sin}}{\mathrm{MSE}_{\sin} + \mathrm{MSE}_{\mathrm{tri}}} \qquad (5)$$

When I_C with values close to 0 this indicate non-stiction while I_C values close to 1 indicate strong stiction. When I_C = 0.5 the method is unable to determine or rule out the presence of stiction.

3.3 Rectangular fitting method

The method presented by Hägglund (2011) evaluates the best match between a sine wave or a square wave and the oscillating control error signal. In order to be able to handle a signal that has no constant characteristics or constant shape, the algorithm uses the information contained between consecutive zero crossings. Stiction in self-regulating processes typically produces rectangular oscillation, which coincides with the main assumption of the algorithm. However, in integrating control loops the typical stiction shape is triangular and thus, the rectangular fitting procedure cannot be applied directly. Nonetheless, it is still possible to use this method on integrating loops as long as the control error data is pretreated with a suitable high-pass filter before implementing the algorithm as demonstrated by Hägglund (2011). The shape matching mechanism used in this method is based on the integral absolute error (IAE). To determine the best match for the shape of the control error signal deviations are calculated using the loss functions:

$$V_{sine} = \sum_{i=1}^{n} \left(e(t_i) - a_{sine} sin\left(\frac{2\pi}{t_p} ih \right) \right)^2 \qquad (6)$$

and

$$V_{square} = \sum_{i=1}^{n} \left(e(t_i) - a_{square} \right)^2, \qquad (7)$$

where h is the sampling period $e(t_i)$ is the control error signal, and n is the number of samples in the interval between zero crossings. When $V_{square} < V_{sine}$, it can be assumed that stiction is the cause of the oscillations. If this is not the case, then the oscillations are caused by an external disturbance or because of controller tuning issues. Consequently the stiction index I_R can be defined as

$$I_R = \frac{V_{sine} - V_{square}}{V_{sine} + V_{square}} \qquad (8)$$

The stiction index I_R can have values between -1 and 1, with positive values indicating stiction.

The stiction index is calculated for each half period of the oscillation. However, the index value may significantly vary for each half period. Thus, the final diagnosis decision is taken using the mean of the I_R values obtained for the analyzed period of time. If the variation in the index value is significant enough, the final diagnosis results may be skewed, which may not reflect the reality of the analyzed signal.

3.4 Bicoherence method

The method presented by Choudhury (2004) is based on determining non-linearity in the process using higher-order statistics, namely the squared bicoherence defined as follows:

$$bic^2(f_1, f_2) := \frac{\left|B(f_1, f_2)\right|^2}{E\left\{\left|X(f_1)X(f_2)\right|^2\right\}E\left\{\left|X(f_1+f_2)\right|^2\right\}+\varepsilon} \qquad (9)$$

where $B(f_1,f_2)$ is the bispectrum of the tested signal and ε is a small constant. For selecting a suitable ε, please refer to Choudhury (2006). To test the nonlinearity of a signal, two tests are required. The first evaluates whether the squared bicoherence $bic^2(f_1, f_2)$ is zero for all frequencies f_1 and f_2, indicating a Gaussian signal. If the signal is non-Gaussian, i.e. $bic^2(f_1, f_2)$ is non-zero, it is tested for non-zero constant squared bicohence, to find out if the signal is nonlinear. Two indices representing these tests have been defined by Choudhury (2006). The non-Gaussianity index (NGI) is defined as:

$$NGI := \frac{\sum bic^2_{significant}}{L} - \frac{C_\alpha^{\chi^2}}{2K} \qquad (10)$$

where $bic^2_{significant}$ represents the bicoherence values that exceed the limit value $c_\alpha^{\chi^2}$, L is the number of $bic^2_{significant}$, and K is the number of data segments used in the bicoherence estimation, see e.g. Choudhury (2004). The non-linearity index NLI is defined as

$$NLI := bic^2_{max} - \left(\overline{bic^2_{robust}} + 2\sigma_{bic^2,\, robust}\right) \qquad (11)$$

where $\overline{bic^2_{robust}}$ and $2\sigma_{bic^2,\, robust}$ are the robust mean and the robust standard deviation of the estimated squared bicoherence, respectively. These parameters are calculated by neglecting the smallest and largest 10% of the bicoherence values.

Both indices, NGI and NLI, are bounded between -1 and 1 and positive values of NGI and NLI indicate non-Gaussianity and non-linearity, respectively.

3.5 Reliability indexing for weighting diagnosis results

The introduction of a reliability index for the stiction diagnosis algorithms aims to define the degree of certainty of the diagnosis decision. However before defining the reliability index it is necessary to consider two issues. First, a method is able to provide trustworthy results only if the assumptions behind the method hold. In particular, the usual requirements of the stiction diagnosis methods are the presence of clear oscillations and the stationarity of the process data. In addition, some methods are applicable only if the process under consideration contains or does not contain integration. These listed assumptions should be tested for each stiction detection method and summarized in its applicability index a_i.

Secondly, even if all the assumptions of a method are fulfilled, the decision of the method may be uncertain because of process noise, disturbances propagating from other loops and the presence of a small-magnitude stiction. This second part of the reliability index (the resolution index) must represent the degree of matching of the process data to one of the patterns related to healthy or stiction valve cases. In other words, the resolution index has a high value if the method can clearly classify the valve as healthy or under stiction, and the resolution index is low in the opposite case when the process data cannot be described satisfactorily.

Assuming a normal distribution of the fitting errors, the resolution index (degree of certainty) of the decision can be represented in terms of the following likelihood ratios:

$$L_i = logp_i(1)/p_i(0) = (d_i(0) - d_i(1))/2\sigma^2,$$

if $D_i = 1$ and (12)

$$L_i = logp_i(0)/p_i(1) = (d_i(1) - d_i(0))/2\sigma^2,$$

if $D_i = -1$,

where $d(1)$ and $d_i(1)$ are the fitting errors for the faulty and healthy pattern respectively, $p_i(0)$ and $p_i(1)$ are the probability densities of the process data in the case of a healthy and a faulty valve respectively, and D_i is the decision of the method. Equation (12) can then be aggregated to form the combined reliability index of the group of methods in the following way:

$$L = \log \frac{\prod_i p_i(1)}{\prod_i p_i(0)} = \sum_i D_i L_i. \qquad (13)$$

The drawback of the proposed index (13) is that it can produce high values even when the process data can be fitted to neither a faulty nor a healthy pattern and when both $d(0)$ and $d(1)$ are high. Therefore, in order to obtain a reliable diagnosis the following alternative resolution index is proposed and used in this paper:

$$r_i = 1 - 2\frac{\min(d_i(0), d_i(1))}{d_i(0) + d_i(1)}. \tag{14}$$

Summarizing the applicability and resolution sub-indexes, the diagnosis index can be then calculated in the following way:

$$R = \sum_i D_i \min(r_i, a_i) \tag{15}$$

and the final decision is determined by the sign of the sum in Equation (15):

$D_i = 1$ (there is stiction) if

$$\sum_i D_i \min(r_i, a_i) > 0,$$

and (16)

$D_i = -1$ (there is no stiction) if

$$\sum_i D_i \min(r_i, a_i) < 0.$$

In Equations (15) and (16), the impact of every method is limited by its applicability index, which represents the fact that the results of the method cannot be trusted if the assumptions of the method fail, even if the process data can be fitted to one of the patterns very accurately.

The resolution index for the histogram method can be constructed using the Gaussian and camel fitting errors, so the reliability index is calculated as follows according to equation 17:

$$r_{ih} = 1 - \frac{\min(d_g^2, d_c^2)}{(d_g^2 + d_c^2)} \tag{17}$$

where r_{ih} is the squared 2-norm of the error fitting of the Gaussian distribution and d_c^2 is the squared 2-norm of the error fitting of the Camel distribution. r_{ih} is a resolution index with values from 0 to 1; the closer the value is to 1, the more reliable the stiction index can be considered.

In the curve fitting method, the stiction index may provide inaccurate results when the MSE of both sinusoidal and triangular signals is unable to match the original signal. Thus, the resolution index is constructed using the fitting residual of both signals. According to (14), it can be calculated in the following way:

$$\rho_{ic} = 1 - 2\frac{\min(d_{sin},\ d_{tri})}{d_{sin} + d_{tri}} \qquad (18)$$

where d_{sin} and d_{tri} are the fitting errors of the sinusoidal and triangular signal respectively and ρ_{ic} is the resolution index for the curve-fitting method. ρ_{ic} can have values from *0* to *1*; the closer the index value is to *1,* the more reliable the stiction index result can be considered.

The resolution index of the rectangular fitting method employs the values of the sine and square loss functions, since functionally they are similar to the fitting errors used in the histogram and curve fitting methods. Following eq. 14 the resolution index can be calculated as follows:

$$\rho_{ir} = 1 - \left(\frac{\min\left(V_{sine}, V_{square}\right)}{V_{sine} + V_{square}}\right), \qquad (19)$$

where ρ_{ir} is the resolution index for the rectangular fitting method with a range of values from *0* to *1.* ρ_{ir} values above *0.5* are considered reliable, so therefore values below *0.5* are considered unreliable

In terms of reliability, the most important feature of the data for the bicoherence based nonlinearity indices is the stationarity of the data. To estimate the skewness of the data distribution, the mean and the standard deviation of the data must remain constant over the calculation period. This requirement is however seldom achieved when using real industrial data, even after it has been pre-processed. To this end, a reliability index was defined for the NGI and NLI computation. Standard statistical tests, Student's t-test and χ^2-test are used to calculate the mean and the standard deviation, respectively. To compute of the reliability index, the data is divided into *l* segments for which the mean $\bar{x}_i$ and standard deviation σ_i are calculated and tested against the null hypothesis $\bar{x}_i = 0$ and $\sigma_i = 1$. The reliability index R_{BIC} is defined as follows:

$$\rho_{BIC} = \rho_{\bar{x}} \cdot \rho_{\sigma} \qquad (20)$$

where

$$r_{\bar{x}} = 1 - \frac{\#\left\{ \bar{x}_i \;\middle|\; |T_i| > T_{lim} \right\}}{l} \qquad (21)$$

and

$$r_s = 1 - \frac{\#\left\{ s_i \mid c_i^2 < c_{lim,l}^2 \text{ or } c_i^2 > c_{lim,u}^2 \right\}}{l}, \qquad (22)$$

In the above, $T_i = \dfrac{\bar{x}_i}{s/\sqrt{n}}$ is the t-statistic for testing the mean of the data segment *i*, T_{lim} is the limit for the confidence level of 0.05. The variable $c_i^2 = \dfrac{(n-1)s_i^2}{s^2}$ denotes the test statistic for testing the standard deviation for the data segment *i*, while $c_{lim,l}^2$ and $c_{lim,u}^2$ are the lower and upper limits for the confidence level of 0.05. The operator $\#\{\ \}$ takes the number of elements in the set.

4 Description of the Case Studies

The integrated FDD system was tested employing data from four critical control loops of an industrial paperboard machine: The pressure control loop in the second drying group, a flow control loop in the birch dosing, the pressure difference loop in the steam group 8 and a stock mixing flow loop. The loops are located in the drying and the stock preparation sections of the machine. The operational data was gathered from the months of January to June of 2011. Figure 5 shows the controlled variable behavior for each test case.

The first case was a pressure control loop in the second drying group. Figure 5 (first panel) showed monitored data for the month of February. The signals clearly showed that the controlled variable and controller output signal in the loop were oscillating. The maintenance reports described the valve in this loop as “sticky” and the oscillation shape of the signal coincides with the expected behavior of stiction in an integrating process.

The second case was a flow control loop in the birch dosing. The loop was clearly affected by a disturbance, but it did not seem to generate strong oscillations as seen in Figure 5 (second panel). Nevertheless, there was still a visible periodic disturbance present. The valve in this loop was reported as having a malfunction.

The third case was a pressure control loop in the drying section. The loop showed clear oscillatory behavior as seen in Figure 5 (third panel). The valve was reported as being stuck at the start of mocement and the control loop signals show clear oscillatory behavior.

The last case was a flow control valve in the stock mixing, where there was a clear disturbance affecting the behavior of the loop, as seen in Figure 5 (fourth panel). This periodic disturbance exhibited interesting behavior. The valve was reported as malfunctioning due to not being able to open properly.

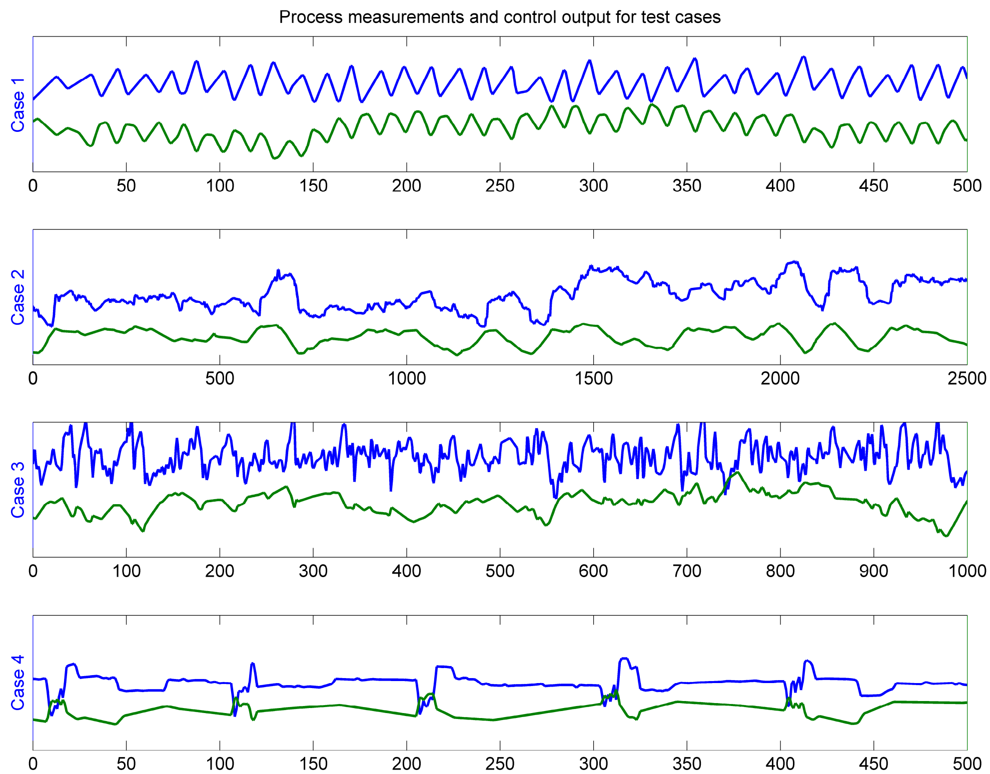

Figure 5: Controlled variable (blue) and controller output (green) signals for each test case

5 Test Results

Each method presented in Section 2 was implemented in the four case studies and tested separately. Next, an integrated FDD system was implemented, where the four stiction diagnosis methods were run in a parallel configuration and weighted according to their reliability indices, and then this system was evaluated.

5.1 Test results of the shape-based stiction diagnosis methods

The diagnosis of the curve fitting method showed high consistency (Figure 6, left top panel) and was able to determine the presence of stiction in most of the case studies tested. However, for some time periods, the method was unable to provide any diagnosis decision. This was related to sudden changes in the shape of the analyzed signal affecting the MSE ratio calculation of the stiction index.

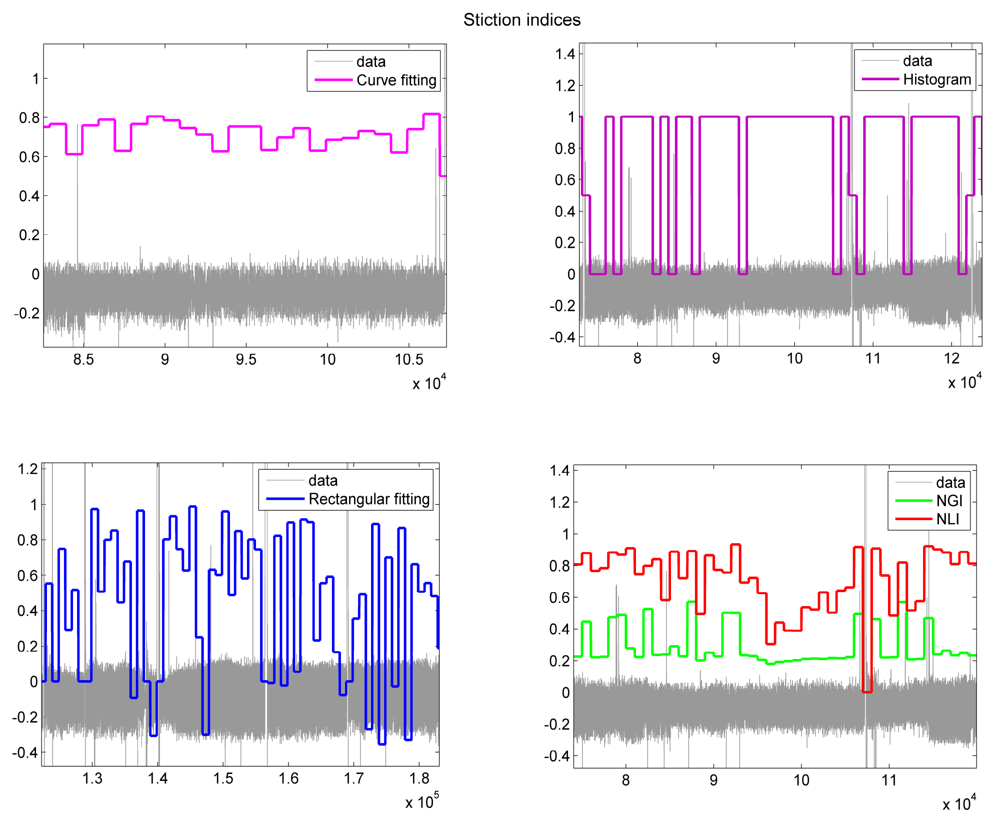

Figure 6: Diagnosis indices for the first study case during the February 2010 period

Figure 7 shows the measurement signal for the first case study tested (top), the histogram of the stiction index (bottom left), the fitting errors for the triangular and sinusoidal functions (bottom right). As seen in Figure 7, the distribution of values of the index is clearly skewed towards values indicating stiction. However, the stiction index values are low, ranging from 0.5 to 0.6. The reliability index, for this case, shows a low value of 0.13, and thus the diagnosis decision cannot be fully trusted. This phenomenon can be seen in Figure 7 (bottom right), where the blue lines indicate the stiction zone, where the fitting error for the triangular signal was significantly lower; the purple lines indicate the no stiction zone where the sinusoidal fitting error is lower; the black lines indicate the zone where no decision could be made since the fitting errors are similar for both functions. The figure shows a number of fitting points in the stiction zone. However, there were also a significant number of fitting points in the no decision zone. The similar fittings were perhaps caused by small disturbances which affected the shape of the signal.

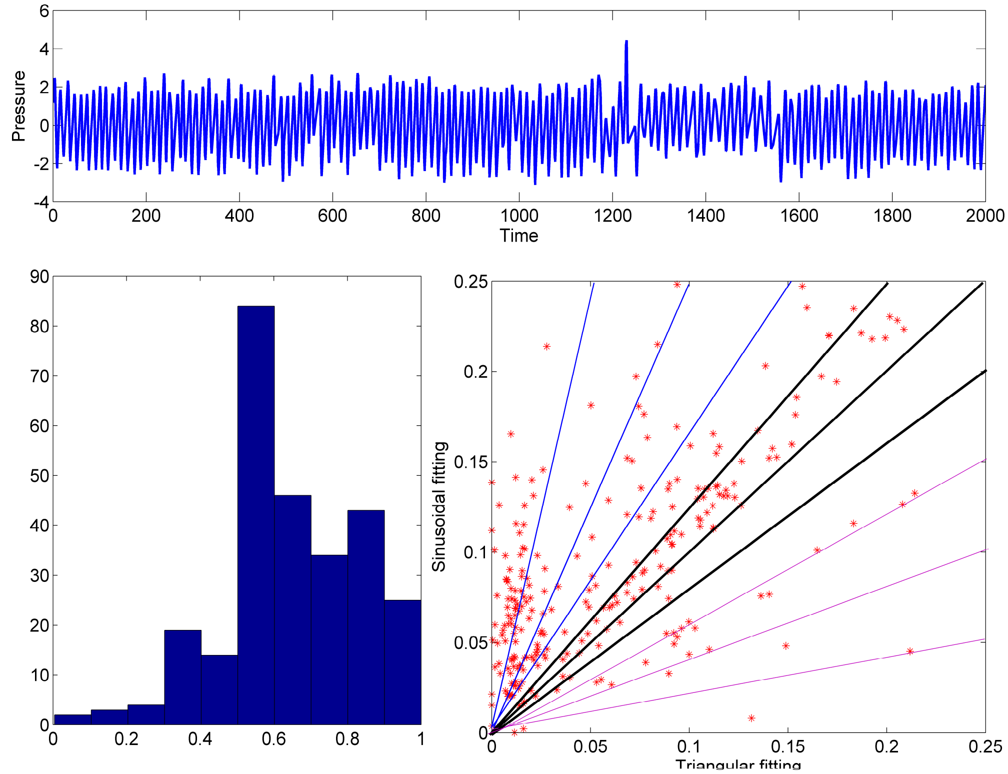

Figure 7: Pressure measurement (top), Index histogram (bottom left), triangular and sinusoidal fitting errors (bottom right)

The results obtained from the histogram method show that the algorithm performed better when implemented for long periods of time. This is logical due its use of a data histogram to analyze the behavior of the process. However, in certain cases, due to the binary values given by the diagnosis index, its diagnosis behavior can be considered contradictory. This can be observed in Figure 6 (top right), where the diagnosis results change abruptly for consecutive periods of time. This behavior can be explained by studying the characteristics of the data histogram constructed by the method. Figure 8 shows the data histogram and the fitted Gaussian and camel distributions. In this example, the data fits better to the Gaussian distribution better and therefore stiction was diagnosed. However, both fittings were similar, and thus the reliability index was low, with a value barely above 0.55. Under these conditions the diagnosis was still considered reliable but not definitive. This phenomenon can occur due to slight alterations in the shape of the data histogram, which are caused by disturbances and noise altering the distribution.

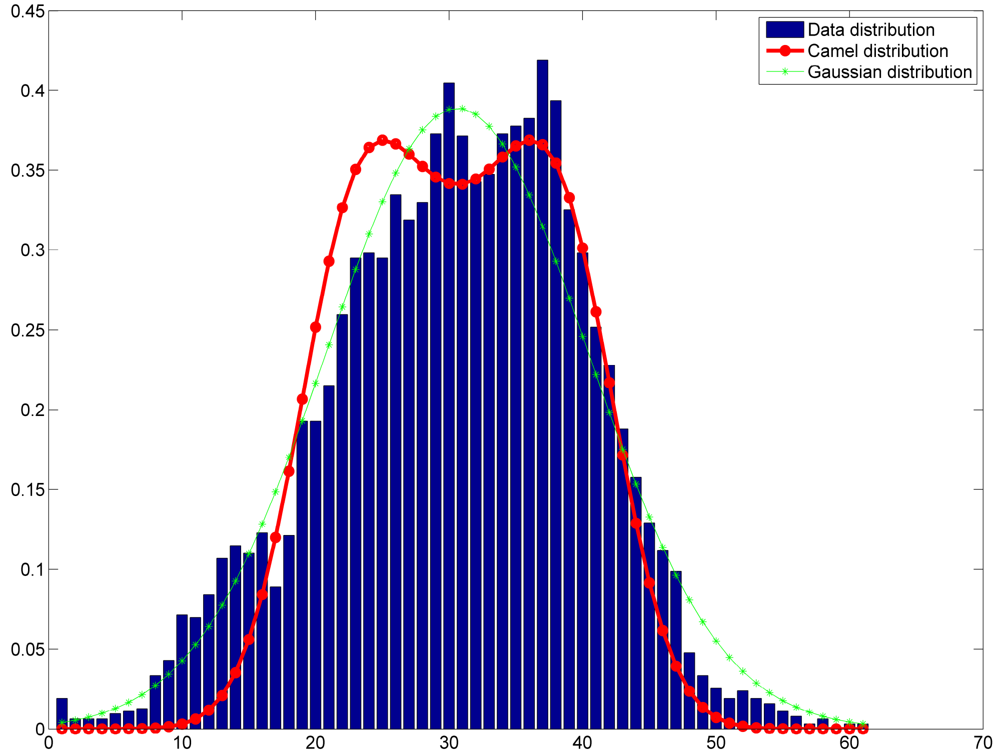

Figure 8: Data histogram, Camel and Sinusoidal signal

The stiction index of the rectangular fitting method showed inconsistent behavior jumping between high and low values (Fig. 6, left bottom panel). This phenomenon was a consequence of the presence of small disturbances or variations in the data, such as sudden changes in the period or amplitude of the oscillation. Nevertheless, in this method, the index values did not reflect the strength or weakness of the stiction, the diagnosis was given by the sign of the index. Thus, the diagnosis of this algorithm can be trusted as long as the index sign remains consistent for consecutive periods. The main source of ambiguity in the diagnosis can come from sudden changes in the sign, which are caused by sporadic disturbances in the signal and the use of the mean value to calculate the stiction index for large periods of time. Figure 9 shows the stiction index distribution (top) and the rectangular and sinusoidal loss functions values for each half period (bottom). In this example, the overall stiction index had the value of -0.10 and the reliability index had the value of 0.57. The low value obtained by the reliability index was related to the high variance shown in the sinusoidal loss function and the triangular loss function. Figure 9 shows that the sinusoidal and rectangular loss functions have relatively high variance, causing significant variation in the stiction index. In addition, the peaks in the loss functions bias the mean stiction index.

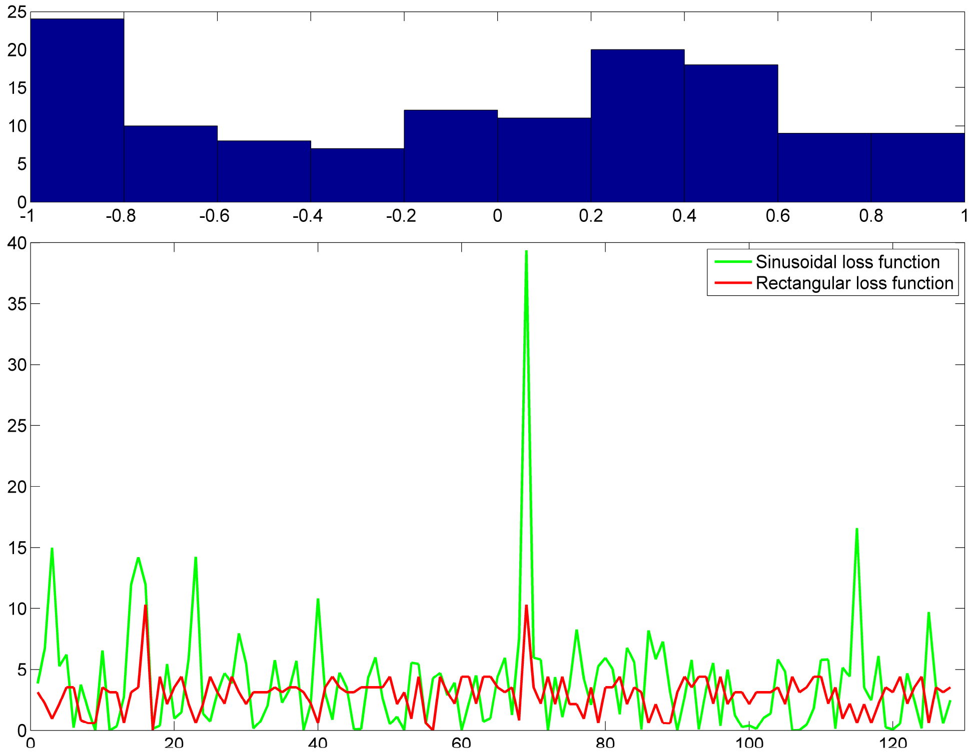

Figure 9: Index histogram (top), rectangular loss function (bottom, red) and sinusoidal loss function (bottom, green)

5.2 Test results of the non-linearity measures based on bicoherence

The bicoherence-based indices also exhibited high consistency in the results (Figure 6 right bottom panel). However, it must be noted that the process in question was not linear and a certain degree of nonlinearity was constantly present.

The variations in the results can be explained by variations in the data, such as small disturbances that distort the data distribution. Since NGI and NLI both measure high-order statistics, they are significantly affected by abnormal values, for example. This is illustrated in Figure 10, which displays three data segments in the February data set. The signals are assumed to represent similar stiction behavior, but the corresponding NGI and NLI values are very different. The corresponding reliability indices for the NGI and NLI values in the three data segments are 1, 0.81 and 0.4, respectively, from top bottom in Figure 10, which indicates that the skewness of the data distribution is clearly affected by the changes in the mean and variance of the data.

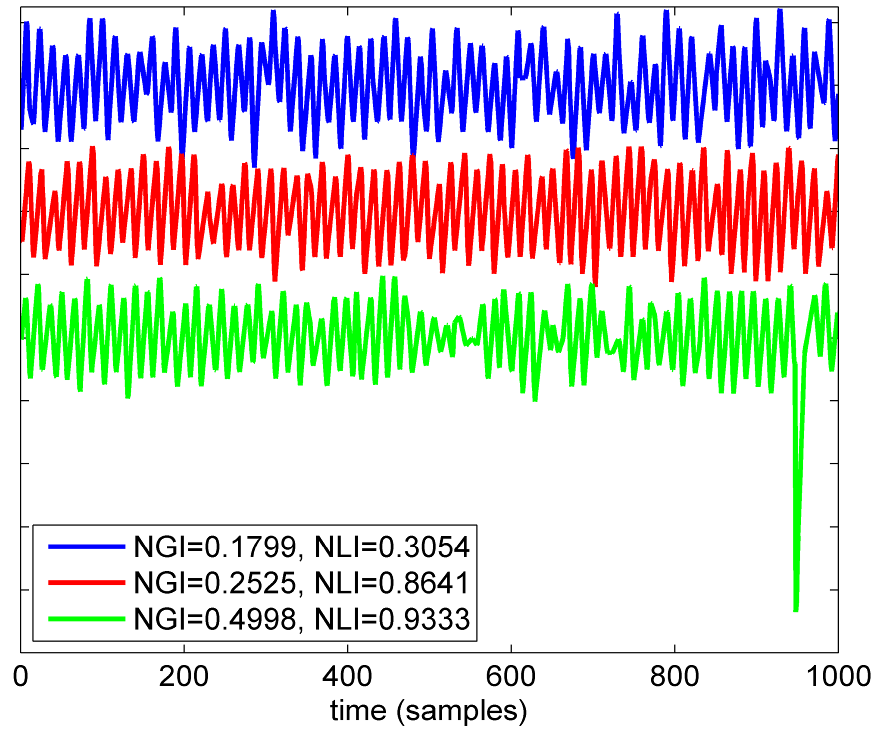

Figure 10: Analysis of bicoherence-based nonlinearity indices and their variations

Table 2: Resulting stiction indices

Test cases & maintenance description	Month	Curve fitting stiction index	Histogram stiction index	Rectangular fitting index	Bicoherence NGI	Bicoherence NLI	Integrated index
Case 1:	January	0.59	0	-0.04	0,21	0.46	0,54
Sticky valve	February	0.71	1	0.17	0,21	0.87	0,65
	March	0.67	1	0.21	0,20	0.67	0,64
Case 2 :	January	0.56	0.5	0.49	0,22	0.45	0,64
Malfunction	February	0.6	1	0.44	0,22	0.41	0,44
	March	0.55	1	0.43	0,21	0.50	0,58
Case 3:	January	0.59	1	0.60	0,19	0.56	0,50
Sticky valve	February	0.58	1	0.51	0,19	0.47	0,49
	March	0.58	1	0.41	0,19	0.69	0,44

Case 4:	January	0.50	1	0.13	0,29	0.22	0,61
Malfunction	February	0.57	1	0.43	0,21	0.41	0,55
	March	0.54	1	0.40	0,27	0.43	0,84

5.3 Test results of the integrated FDD system

The integrated FDD system was tested with the case studies reported in Section 4. The results obtained by using the integrated diagnosis index showed that the use of the reliability indices proposed in Section 3.5 was effective in combining and weighting the diagnosis decisions of the previously tested algorithms, providing a more robust and stable diagnosis than the ones provided by any of the individual stiction FDD algorithms .

The behavior of the integrated system was constant without any sudden changes in its diagnosis and in accordance with the fault information found in the maintenance reports. Figure 11 shows the integrated FDD system stiction index (top) and the analyzed data (bottom). The variations in the value of the integrated index were small and did not alter the overall diagnosis.

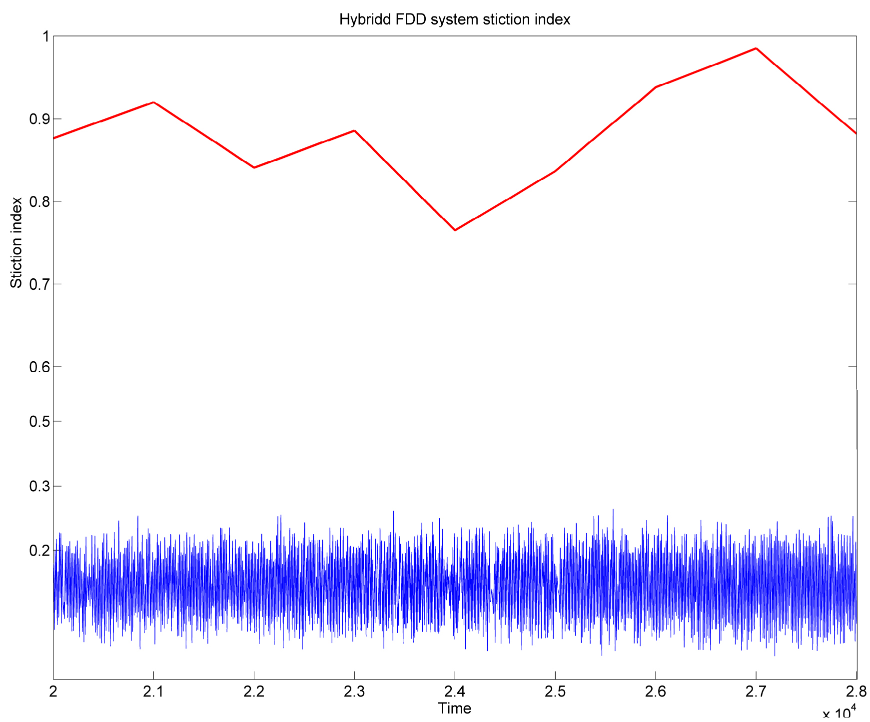

Figure 11: Integrated FDD system stiction index for the first study case during the February 2010 period

5.4 Comparison of the stiction FDD algorithms

The diagnosis indices of the individual methods showed all the methods provided similar diagnoses in the cases in which the oscillation was strong. However, there were some periods of time where the methods did not agree on the diagnosis. Table 2 summarizes the diagnosis indices produced by means of each individual method and the integrated FDD system for all the testing cases.

However, the results shown in Table 2 are unable to capture the dynamic behavior of the methods, which is illustrated in Figure 6. The figure makes it possible to observe small and large variations in the stiction indices caused by each algorithm's false diagnoses or performance issues.

Nevertheless, by analyzing the results of Table 2 it is possible to see contradictory diagnoses in various cases. In comparison, the diagnosis index of the integrated system showed more consistent results.

Figure 11 shows the stiction index of the integrated FDD system proposed in this work. By comparing the behavior of any of the individual diagnoses indices presented in Figure 6 and the integrated FDD system (see Fig. 11), it is possible to observe that the dynamic behavior of the integrated system is more stable than that of the rectangular fitting index and the bicoherence indices. Furthermore, the integrated system's diagnosis index is more definite than that of to the curve fitting method and it does not contain sudden contradictory diagnoses like that of the histogram method.

6 Conclusions

In this work, an integrated FDD system for valve stiction was developed in which different algorithms were implemented to be run in a parallel configuration. Reliability indices for each method were proposed to facilitate the combination of the individual diagnoses. The integrated FDD system was tested with industrial data from a board machine and its performance was compared to the performances of the individual methods.

The results show that an integrated valve stiction FDD system was able to overcome the drawbacks of the individual methods and to form a combined stiction index with more robust and consistent decisions in an industrial environment. The obtained results were also in line with the maintenance reports from the paperboard machine studied, which indicates that the proposed system was able to successfully diagnose the presence of stiction.

The reliability indices were shown to successfully measure the diagnosis uncertainty of the individual stiction detection algorithms in the presence of small disturbances. These indices were then used to determine the importance of the corresponding methods in the final diagnosis by weighting the individual results. As a result, the diagnosis decision of the integrated FDD system was able to take into account the diagnosis indices of the methods, providing a robust and unified diagnosis.

The proposed FDD system is scalable, modular and can be implemented for online use in plants, where it could provide the plant operators valuable information about the state of the control loops.

In a future study, the computational load of the integrated system can be reduced, which is currently high due to the parallel computation of the stiction and reliability indices. In addition, the overall performance of the system can be further improved by introducing different types of valve stiction detection algorithms.

Acknowledgment

The research leading to these results has received funding from the European Union Seventh Framework Programme (FP7/2007-2011) under grant agreement n° 257580

References:

Bendat P., Piersol AG. (1971), *Random data: Analysis and measurement procedures*. Wiley, New York.

Choudhury, M.A.A.S., Shook D. S., and Shah S.L., (2006), Linear or Nonlinear? A bicoherence based metric of Nonlinearity measure, *Proceedings of IFAC-Safeprocess 2006 Symposium, Beijing,* Zhang Zhang pp. 617–622

Ender, D.B. (1993), Process control performances. Not as good as you think. *Control Engineering, 40*, pp. 180–190

Hägglund, T. (2011), A shape-analysis approach for diagnosis of stiction in control valves, *Control Engineering Practice 19*, pp.782-789.

He, P., Wang, J., Pottmann, M., Qin, J. (2007), A curve fitting method for detection valve stiction in oscillating control loops, *Industrial and Engineering Chemistry Research 46*, pp. 4549-4560

Horch, A. (1999), A simple method for the detection of stiction in control valves, *Control Engineering Practice, 7*, pp.1221-1231.

Horch. A. (2006a), Method and a system for evaluation of static friction, *US patent 7047152*, http://www.freepatentsonline.com/7047152.html

Horch A., (2006b), "Benchmarking control loops with oscillations and stiction" in Process Control Performance Assesment: From theory to implementation, eds, Ordys A., Uduehi D., Jonhson M., Springer-Verlag New York; edn,pp 227-257

Isermann R. (2011), *Fault diagnosis applications*, Springer, Berlin, pp. 122-139.

Jelali, M., & Huang,B. (2010), Detection and diagnosis of stiction in control loops—state of the art and advanced method. Springer-Verlag London, pp. 103-265

Jelali, M. & Scali, C. (2010), "Comparative study of valve-stiction-detection methods" in Detection and Diagnosis of Stiction in Control Loops: State of the Art and Advanced Methods, eds. M. Jelali & B. Huang, Springer-Verlag London; edn, pp. 337.

Jämsä-Jounela, S.L., Tikkala, V.M., Laavi, H., Myller, T., Kulomaa, T., Hämäläinen V., (2012), Outline of a fault diagnosis system for a large-scale board machine, *International Journal of Advanced Manufacturing Technology*, pp. 1-15.

Kano, M., Maruta, M., Shimizu, K., & Kugemoto, H. (2004), Practical model and detection algorithm for valve stiction. *Seventh international conference on dynamics and control of process systems* (*DYCOPS7*). Cambridge

Lee, K. H., Ren, Z., Huang, B. (2008), Novel Closed-loop Stiction Detection and Quantification Method via System Identification. 2008 International Symposium on Advanced Control of Industrial Processes. Jasper, Canada .

Nallasivam, U., Babji, S., Rengaswamy, R. (2010), Stiction identification in nonlinear process control loops, *Computers & Chemical Engineering 34*, pp.1890-1898.

Rossi, M. & Scali, C. (2005), A comparison of techniques for automatic detection of stiction: simulation and application to industrial data, *Journal of Process Control*, *vol. 15*, no. 5, pp. 505-514.

Singhal, A., Salsbury T.I., (2005). A simple method for detecting valve stiction in oscillating control loops, *Journal of Process Control 15*, pp.371-382.

Scali C., Ghelardoni C., (2008), "An Improved Qualitative Shape Analysis Technique for Automatic Detection of Valve Stiction in Flow Control loops", *Control Engineering Practice, 16*; pp. 1501-1508.

Scali, C. & Farnesi, M. (2010), Implementation, parameters calibration and field validation of a Closed Loop Performance Monitoring system, *Annual Reviews in Control, vol. 34, no. 2*, pp. 263-276.

Stenman, A., Gustafsson F., Forsman, K., (2003), A segmentation-based method for detection of stiction in control valves. *International Journal of Adaptive Control and Signal Processing 17*, pp. 625-634.

Srinivasan, R., Rengaswamy R., Miller R., (2005). Control performance assessment. *Industrial and Engineering Chemistry Research 44*, pp.6708-6718.

Thornhill N. (2005), Finding the source of nonlinearity in a process with plant-wide oscillations. *IEEE Transactions on Control Systems Technology* 13, pp. 434–443.

Yamashita, Y. (2006), An automatic method for detection of valve stiction in process control loops. Control Engineering Practice, 14, pp. 503–510.